Cross-Linking Organic Cathodes Enhances Stability at the Expense of Ionic Accessibility

Ani N. Davis[1†], Kausturi Parui[2†], Mahmudul Hasan[1], Lianett Pineda[2], John Langhout[2], Kiana Treaster[1], Megan M. Butala[2*], Austin M. Evans[1,2*]

[1]George and Josephine Butler Polymer Laboratory, Department of Chemistry, [2]Department of Materials Science and Engineering, University of Florida, Gainesville, FL 32611, USA

Supporting Information

Professor Megan M. Butala
Department of Material Science and Engineering, University of Florida
Rhines Hall 172, 1698 Gale Lemerand Drive, Gainesville Florida, 32611
mbutala@ufl.edu

Professor Austin M. Evans
Department of Chemistry, University of Florida
Leigh Hall 402, 1680 Union Road, Gainesville Florida, 32611
austinevans@ufl.edu

Table of Contents

List of Supporting Figures

A. Materials and Methods

Materials

All materials for the network synthesis and model compound synthesis were purchased from Sigma-Aldrich. Deuterated solvents were purchased from Cambridge Isotope Laboratories. All materials were used as received or prepared according to referenced literature procedures. Solvents were dried over 5 Å sieves unless specified otherwise. Reactions were performed under inert reaction atmosphere unless otherwise specified. All reactions were performed using a 100 mL round bottom dried in a 150 °C oven overnight. Materials for electrode casting were purchased from MSE supplies and lithium metal anode were procured from MTI.

Methods and Instrumentation

Nuclear Magnetic Resonance Spectroscopy. All ^{1}H nuclear magnetic resonance (NMR) spectra were collected on a Brucker 400 MHz spectrometer at 298 K. ^{13}C NMR spectra were acquired using a Brucker 400 MHz spectrometer. Chemical shifts were calibrated using residual NMR solvent as an internal reference.

Fourier-Transform Infrared Spectroscopy. Fourier-transform infrared spectroscopy was performed using an Agilent Cary 630 instrument with a diamond attenuated total reflection (ATR) attachment with 1 cm^{-1} resolution in ambient atmosphere. All spectra are shown with atmospheric background subtracted.

Thermogravimetric Analysis. Thermogravimetric analysis was conducted on a TA Instruments TGA550 using platinum sample pans. Samples were heated to 600 °C at a 10°C min^{-1} under Ar//N_2 flow.

Cyclic Voltammetry. Cyclic voltammetry was collected using a Bio-Logic SP-50e potentiostat with a three-electrode set up: Pt as the working electrode, Pt wire as the counter electrode, and a Ag wire reference electrode. Samples were measured at 0.5mM concentration in dichloromethane with 0.1M *n*Bu_4NPF_6 electrolyte. Ferrocene was used as an internal reference. Measurements were carried out at room temperature under N_2.

Battery Cycling. Batteries were galvanostatically cycled on a Bio-Logic Variable Multichannel Potentiostat VMP3.

Powder X-ray Diffraction (PXRD). PXRD patterns were collected at the University of Florida Nanoscale Research Facility on a Panalytical X'pert Materials Research Diffractometer (MRD) (40 kV, 40 mA) equipped with Cu Kα1 radiation, $\lambda = 1.54056$ Å at room temperature. The patterns were recorded in the 2θ range of 0-45° and the scanning rate was 1.5 s per step with a step size of 0.1° for an overall exposure time of 12 mins.

Scanning Electronic Microscopy (SEM). SEM micrographs were collected using a Tescan MIRA3 at the University of Florida Nanoscale Research Facility. All micrographs were taken in secondary electron imaging mode using an accelerating voltage of 5 kV. All powders were coated with carbon for imaging. A low electron beam current was used to reduce exposure of sensitive samples to the electron beam.

B. Synthetic Procedures

Synthesis of NDI networks

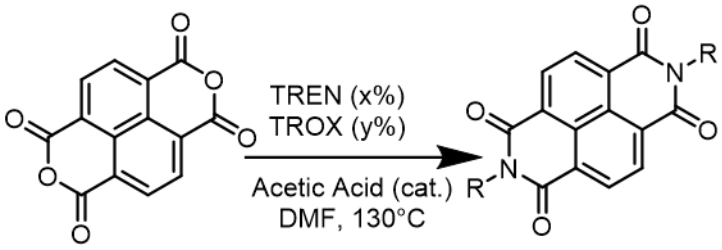

Figure S1. Synthetic Scheme of NDI network synthesis

General Procedure: To an oven dried round bottom flask, naphthalene dianhydride (NTCDA) (2 g, 14.9 mmol) was added with anhydrous DMF (40 mL). The reaction mixture was sparged with N_2 gas and stirred. The reaction mixture was brough to 130 °C. After 30 minutes, TROX and TREN (14.9 mmol total, see eq. S1-3 for amounts) was added via syringe simultaneously to the mixture. The solution immediately turned cloudy upon amine addition. The reaction was heated to 130 °C and stirred for 4 hours. Afterwards, the reaction mixture was brought to room temperature. The solution was poured over a vacuum filter apparatus and washed with water, methanol, isopropanol, and hexanes until the liquid collected was clear. The powder was dried at 150 °C overnight.

FT-IR (Diamond-ATR, cm^{-1}): 3088, 2856, 1702, 1659, 1580, 1456,1375, 1340, 1246, 765

Eq. S1	Anhydride (mmol) / 2 = total amount of amine (mmol)
Eq. S2	(Total amount of amine (mmol) * X%) / 3 = mmol TREN
Eq. S3	(Total amount of amine (mmol) * Y%)/ 2 = mmol TROX

Table 1. Reagents, synthetic yields, and densities of NDI-*X*

NDI-*X*	NTCDA (g)	TROX (g)	TREN (g)	Yield (g, %)	Density (g mL^{-1})
NDI-0	2	1.64056	0	1.88, 55%	1.0
NDI-10	2	1.47651	0.07270	2.16, 66%	0.98
NDI-25	2	1.23042	0.18174	1.99, 63%	0.96
NDI-50	2	0.82028	0.36348	1.22, 42%	1.0
NDI-75	2	0.41014	0.54522	2.17, 81%	1.06
NDI-100	2	0	0.72997	0.83, 34%	1.0

Synthesis of NDI-Model Compound

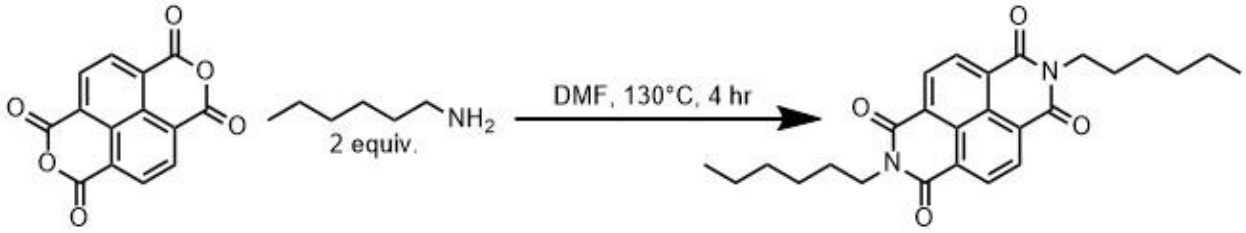

Figure S2. Synthetic Scheme of the NDI Model Compound, NDI-Hexyl

Procedure was adapted from previous literature.[1] 1,4,5,8-Naphthalenetetracarboxylic dianhydride (NTCDA) (1eq, 100mg, .373 mmol) and hexylamine (2 eq , 98.0 microliters, .746 mmol) are placed in a round bottom flask with DMF (20 mL). The mixture was sparged with N_2 for 30 minutes. The mixture was heated to 130 °C and stirred for 4 hours. The mixture was cooled to 0° C in an ice bath. The precipitate was vacuum filtered. The solid was dissolved in dichloromethane and washed with water (3x). The organic layer was dried with sodium sulfate. The liquid was removed under vacuum. Characterization was consistent with previous reports. Yield 113.2 mg (70% yield)

^{1}H NMR (400 MHz, $CDCl_3$) δ 8.74 (s, 4H), 4.30 – 4.06 (m, 4H), 1.73 (s, 4H), 1.49 – 1.33 (m, 12H), 0.94 – 0.83 (m, 6H).

^{13}C NMR (101 MHz, $CDCl_3$) δ 162.63, 130.73, 126.43, 40.80, 31.30, 27.84, 26.55, 22.36, 13.86.

C. Nuclear Magnetic Resonance Spectroscopy

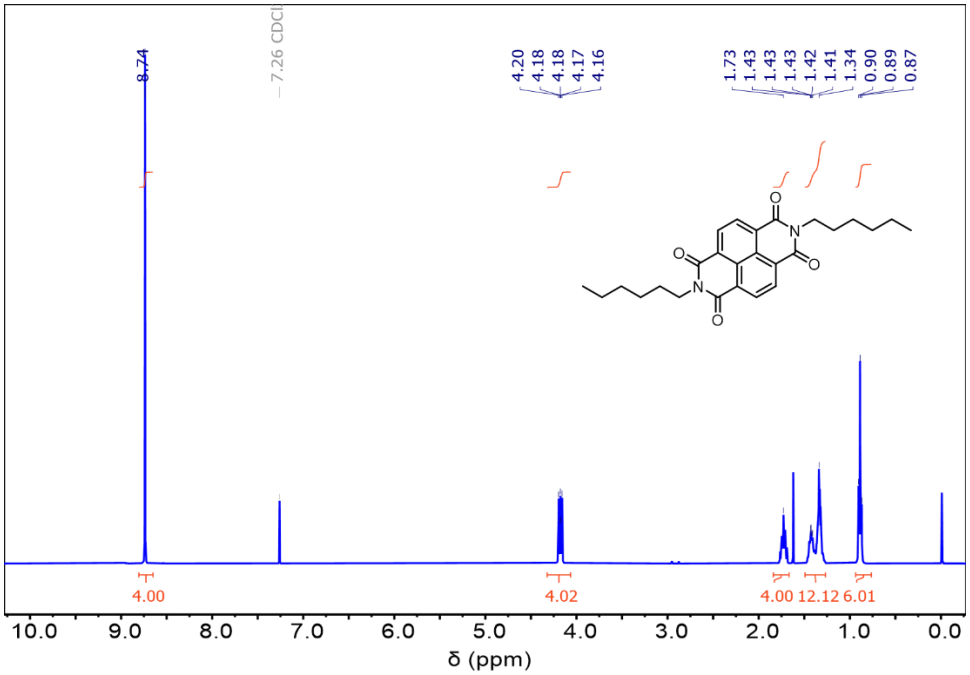

Figure S3. ^{1}H-NMR (400 MHz, $CDCl_3$) of NDI model compound

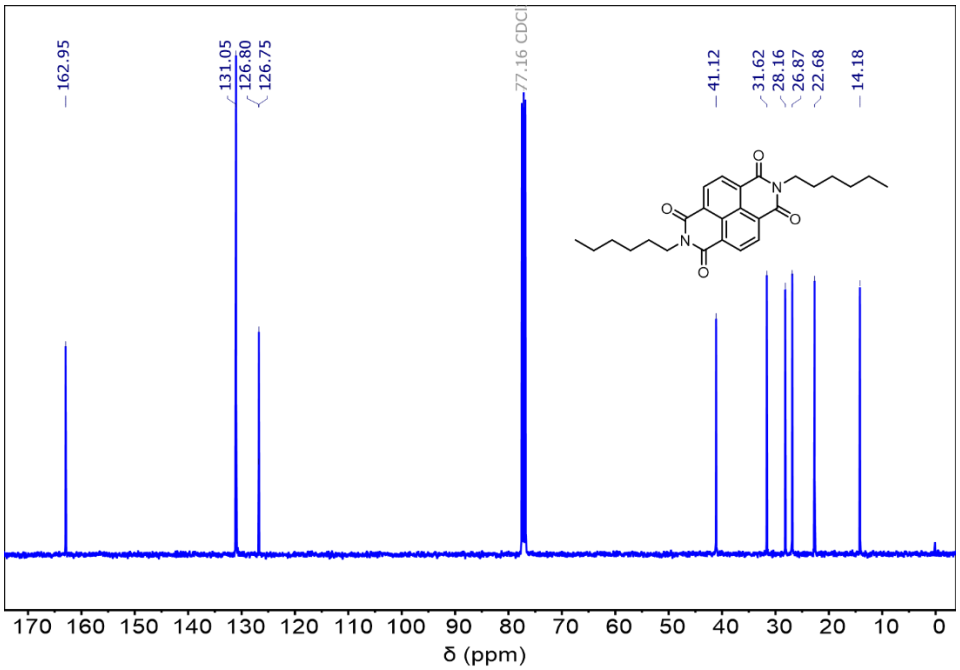

Figure S4. ^{13}C-NMR (101 MHz, $CDCl_3$) of NDI model compound

D. Electrode Fabrication and Coin Cell Assembly

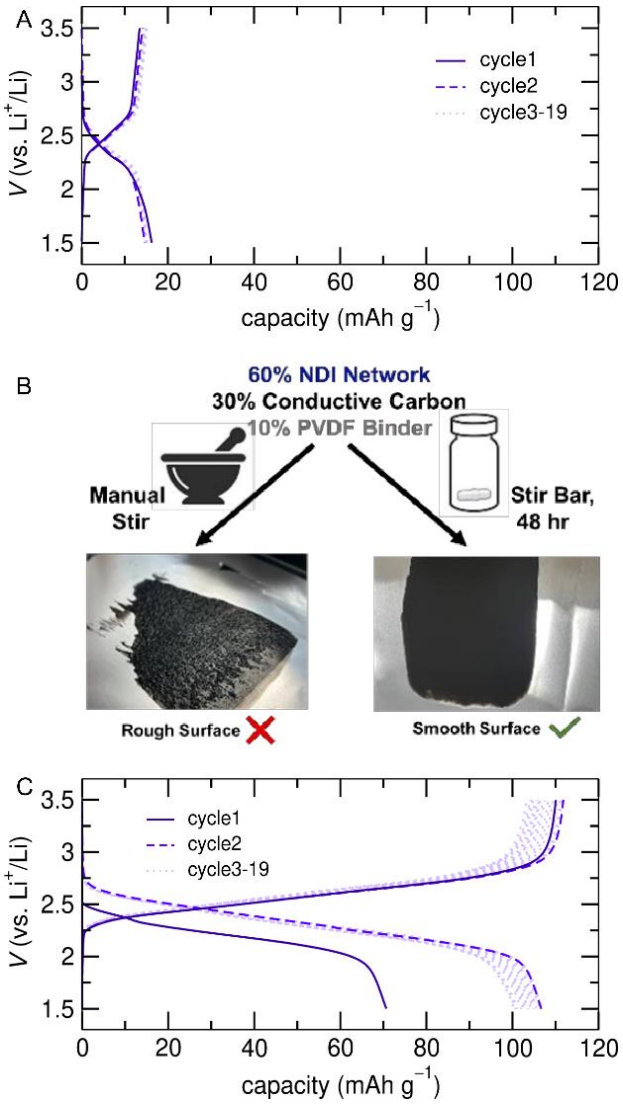

Figure S5. (A**)** GCPL of Swagelok cell of NDI-50. (B) Images of casted composite electrode material. (C) GCPL of Coin cell of NDI-50

Loose powder swagelok cells for GCPL were made with NDI-*X* active material, conductive carbon (Super P) and polytetrafluroroethylene (PTFE) in a mass ratio of 6:3:1, hand mixed in agate mortar and pestle. Loose powder swagelok cells for EIS were made with NDI-*X* active material and conductive carbon (Super P) in a mass ratio of 6:4, hand mixed in agate mortar and pestle. Composite electrodes were made by first vigorously stirring a slurry of NDI-*X* , conductive carbon (Super P, MSE Supplies), and polyvinylidene flouride (PVDF, MSE Supplies) in a 6:3:1 ratio with anhydrous N-methyl-2-pyrollidone as solvent for 48 hours. Casting procedure was adapted from previous literature.[2] The slurry was then cast on aluminum foil (MSE Supplies) using a 15 μm doctor blade and dried at 40 °C for 2 hours on a hot plate. The cast electrodes was further dried at 40 °C in an oven overnight to remove any trace amounts of NMP.

For both cell configurations cells were assembled in an Ar filled glove box using Li metal (MTI, 99.9%) as the counter and reference electrode and a 1M solution of LiPF6 in ethylene carbonate: dimethyl carbonate (1:1 vol) as the electrolyte. Cathode and anode were separated by 2 Whatman glass filter dryer (GFD) disks in swagelok cells, while a porous polypropylene separator (Celgard 2500, 25 μ) was used for coin cells. The thickness of the coin cell NDI-*X* electrodes ranged from 0.9 – 4.3 mg cm^{-2}. EIS was measured at an amplitude of 10 mV and a frequency range from 200 kHz to 100 MHz. The C-rates for both swagelok and coin cells for NDI-*X* cathodes have been based on the reaction of 1 mol of Li and were cycled at the rate of C/10 for all crosslinks from a lower potential limit of 1.5 and an upper limit of 3.5 V. Coin cells of NDI-75 and NDI-25 were also cycled with varying cycling rates of C/10 for 7 consecutive cycles; C/5, C/2.5, 1C,8C, 4C and 2C for 5 cycles and a final set of C/10 for 5 cycles.

E. Pre and Post Formation Cycle EIS of select NDI-*X*

EIS was taken of selected NDI-*X* networks before and after formation GCPL cycles (10 cycles, Rate: C/10).

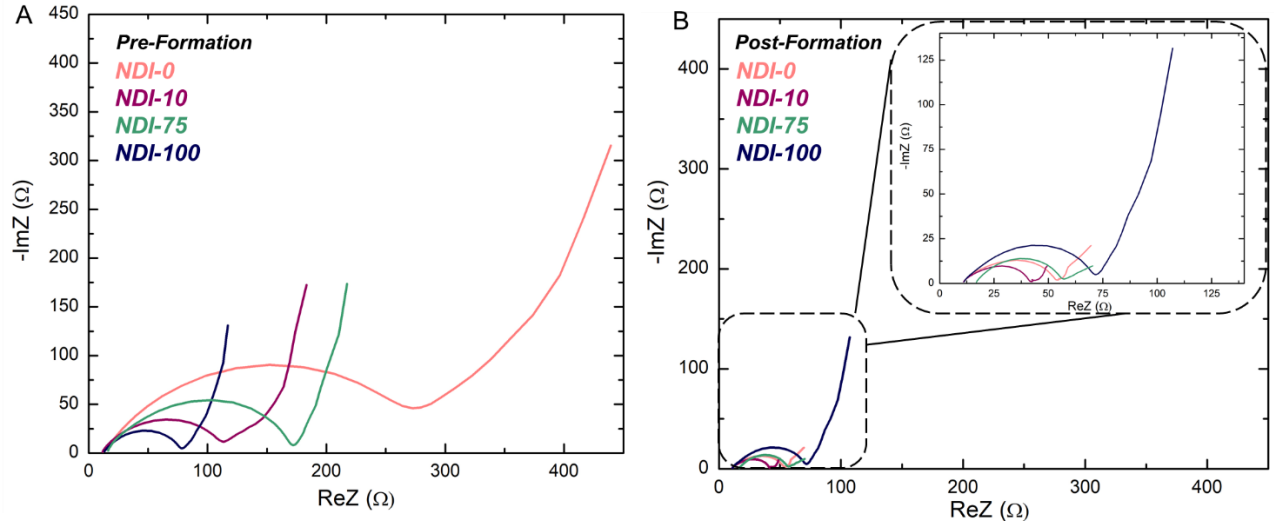

Figure S6. Electrochemical impedance spectroscopy traces of selected NDI-X A. pre-formation and B. post-formation cycles.

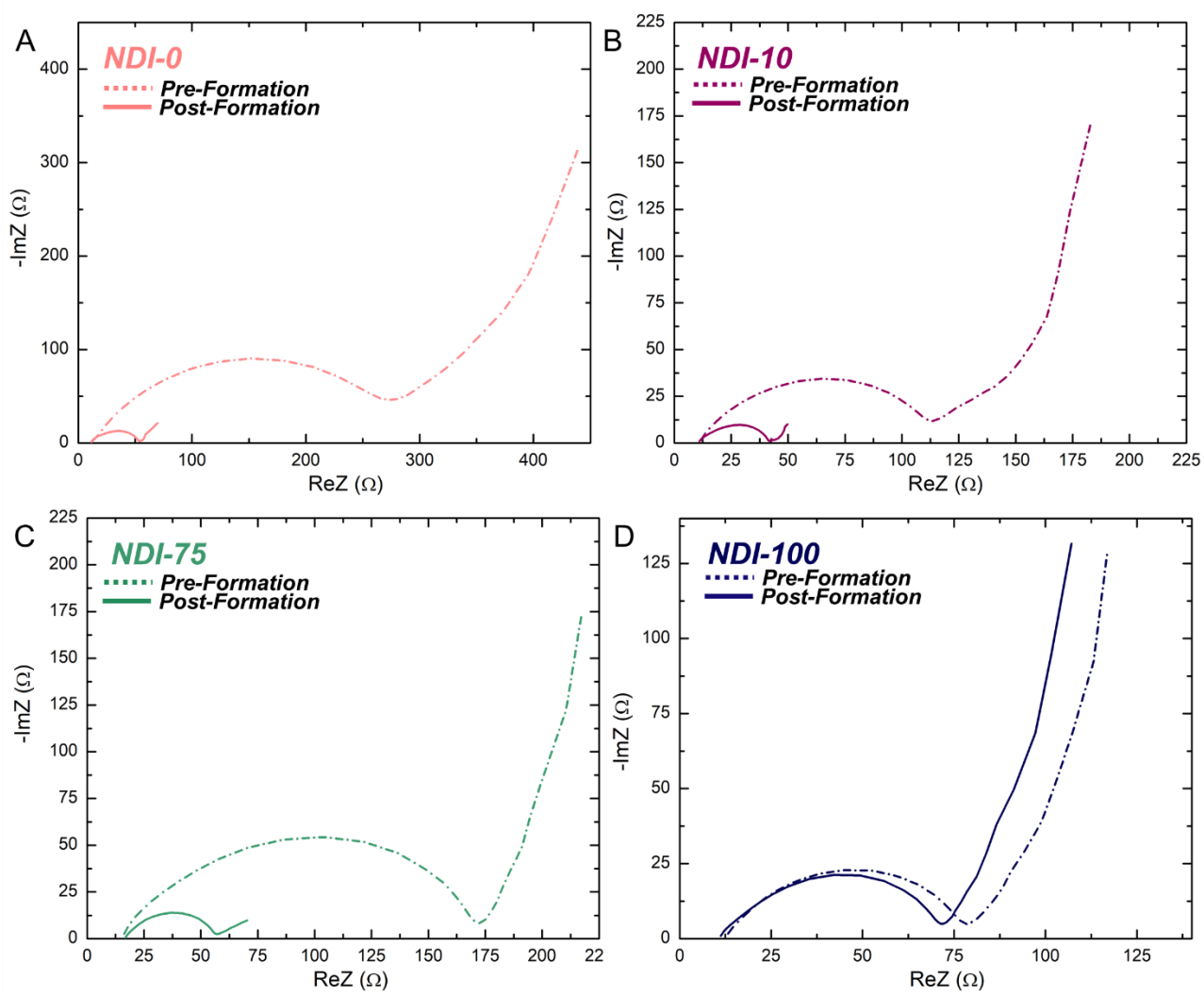

Figure S7. Pre- and Post-Formation EIS of A. NDI-0, B. NDI-10, C. NDI-75, and D. NDI-100

F. Additional Figures

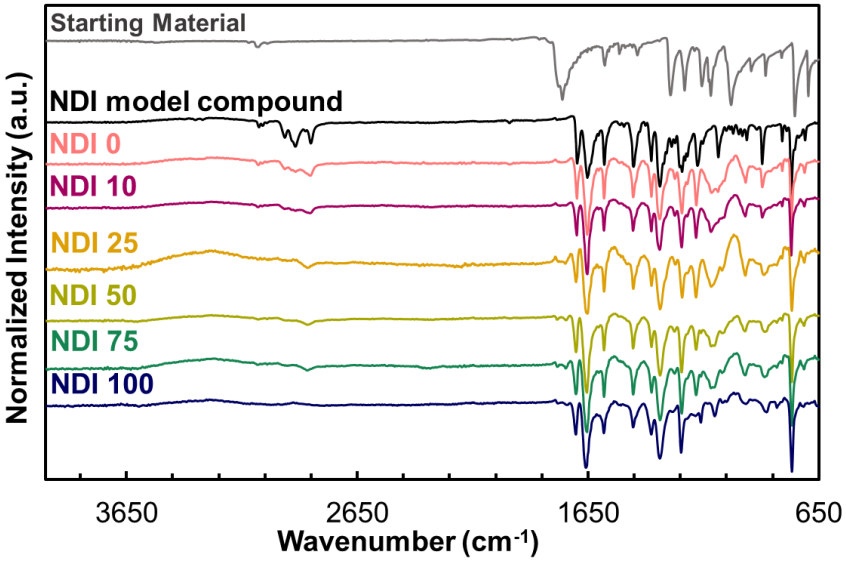

Figure S8. FT-IR of anhydride starting material, NDI model compound, and NDI-*X* networks

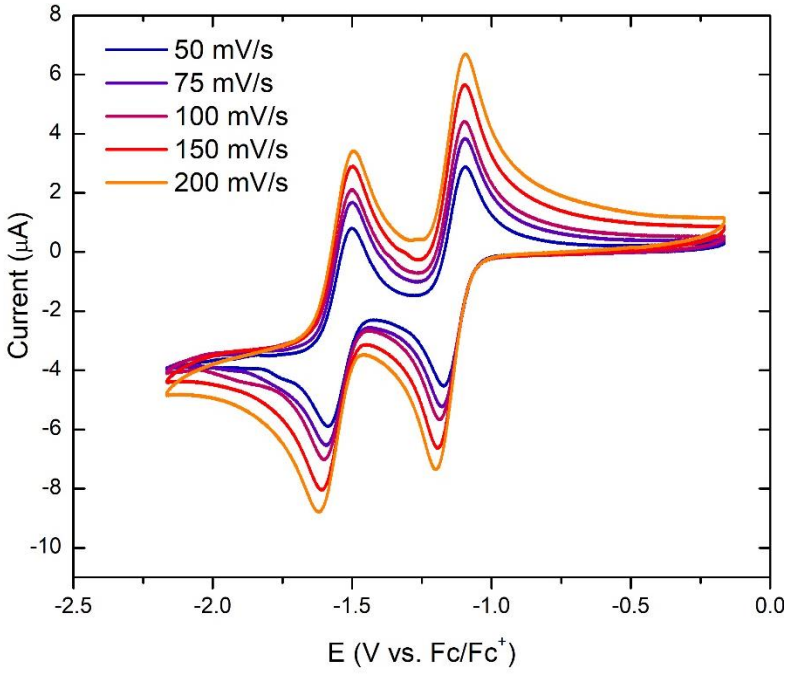

Figure S9. Cyclic voltammetry of the NDI model compound recorded in dichloromethane 0.1M *n*Bu_4NPF_6 electrolyte at variable scan rates

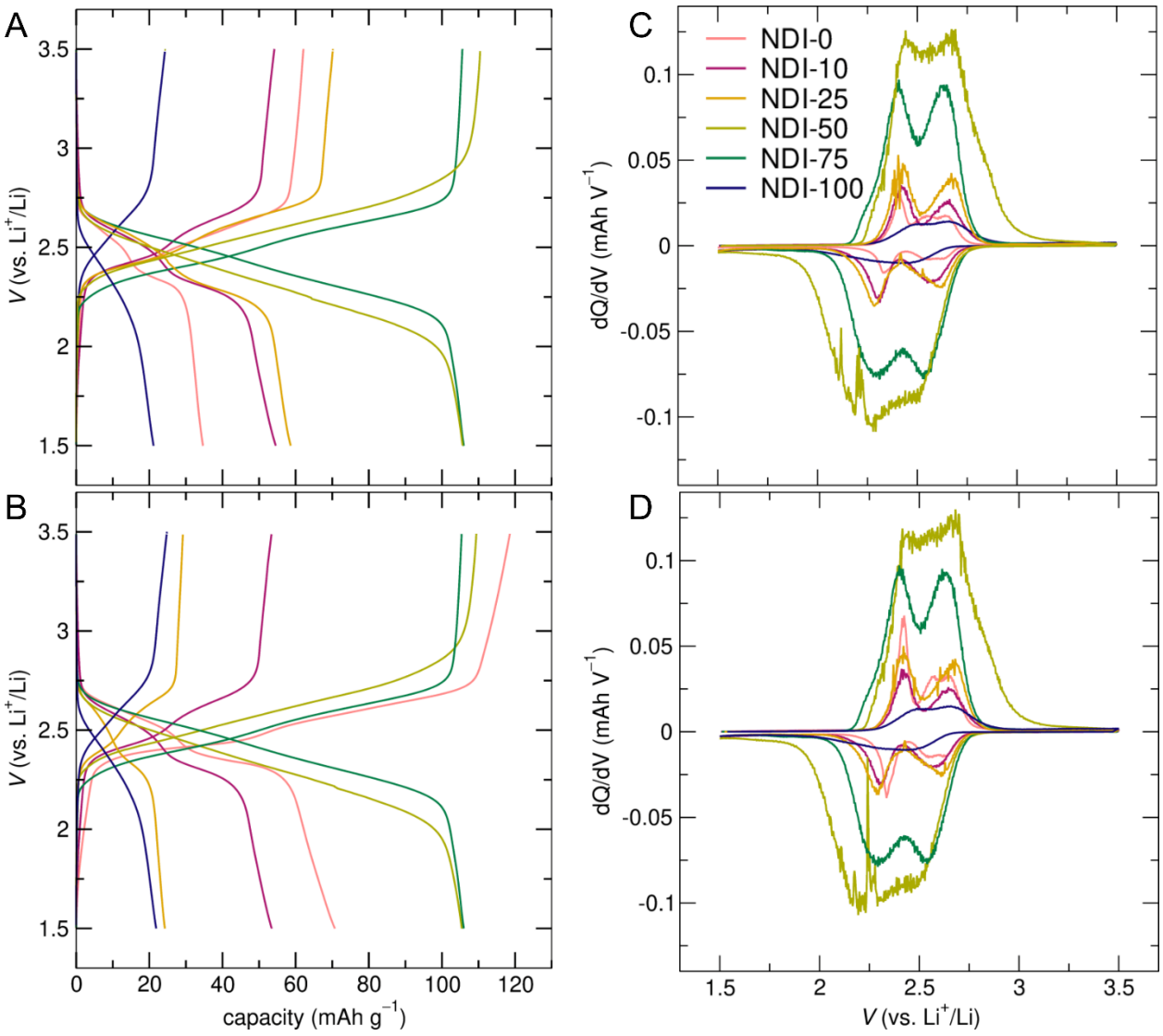

Figure S10. Cycling behavior comparison for different cycle numbers for NDI-*X* cathodes. GCPL shown for (A) cycle 5 and (B) cycle 6 and their corresponding differential capacity plots shown for (C) cycle 5 and (D) cycle 6.

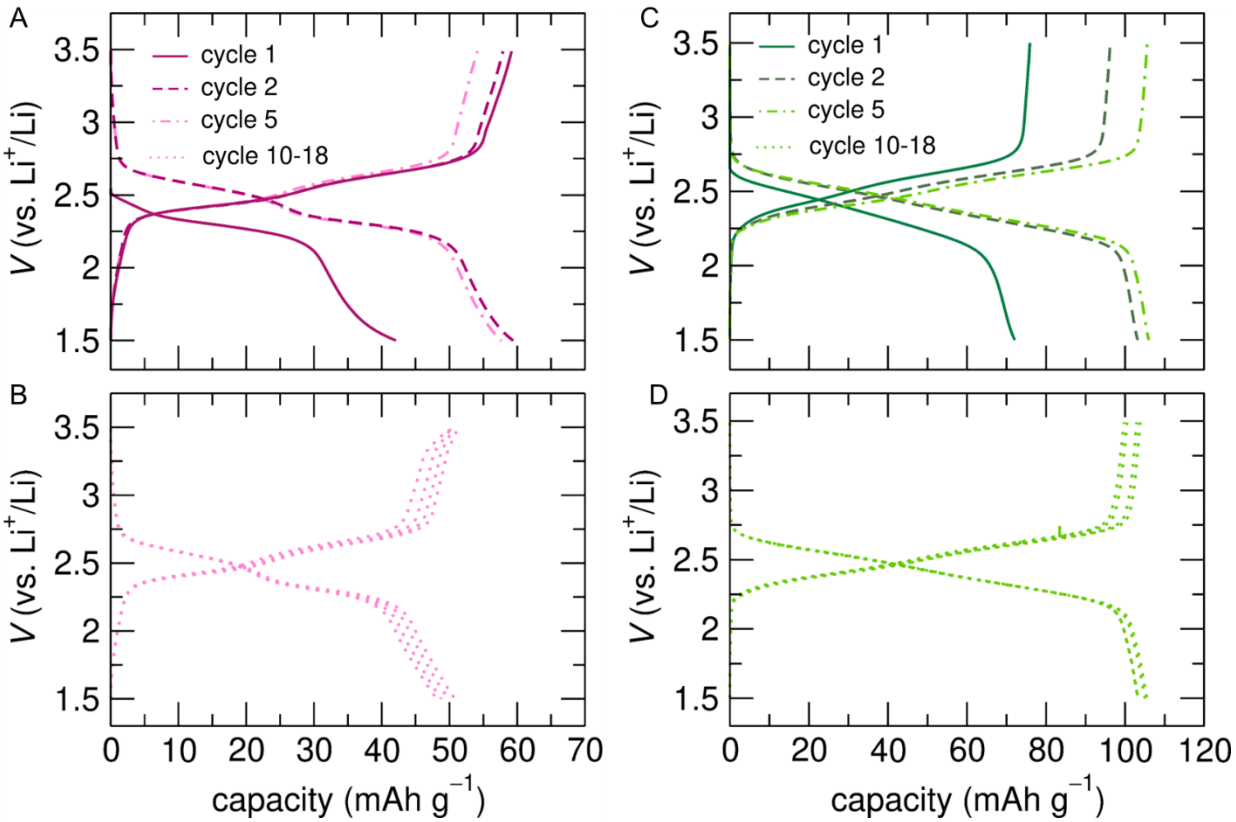

Figure S11. Comparative cathode performance between NDI-10 and NDI-75. The first five cycles of GCPL for (A) NDI-10 and (B) NDI-75 collected a C/10 rate. GCPL of every other cycle for cycles 5-18 for (C) NDI-10 and (D) NDI-75

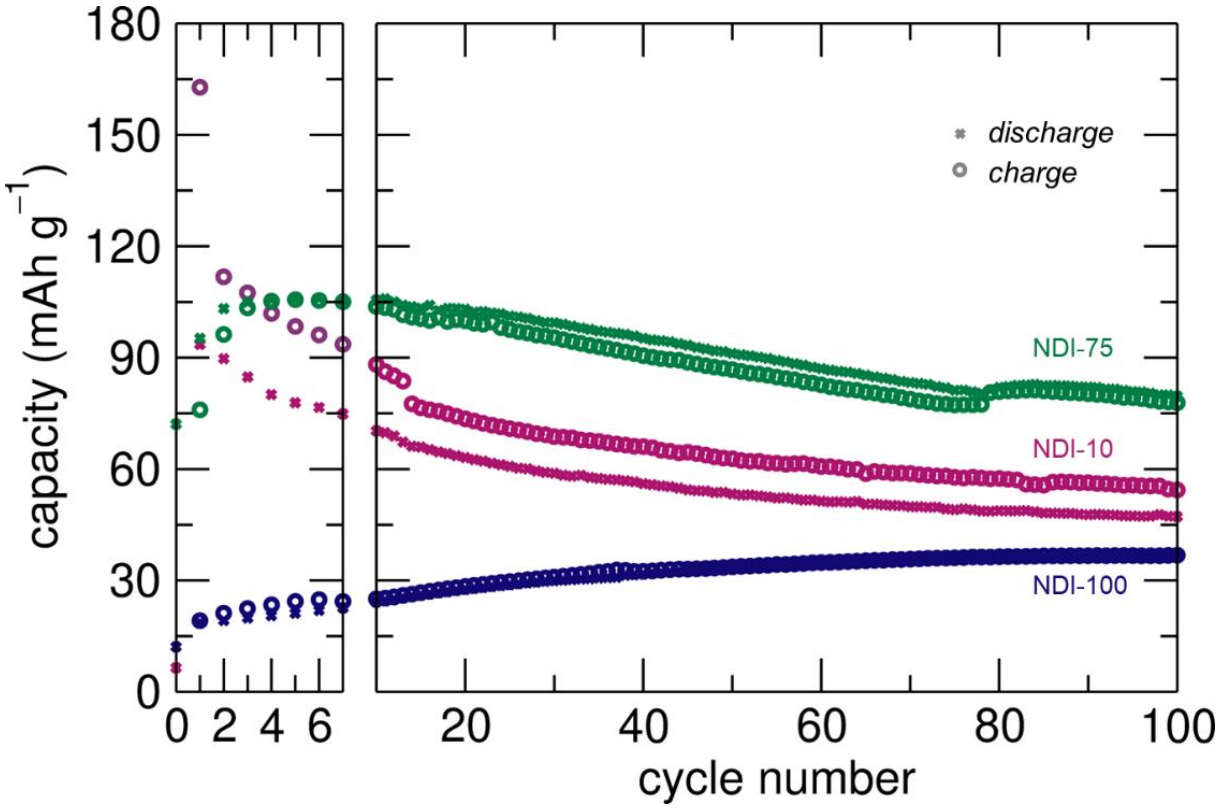

Figure S12. Long-term cycling stability of NDI-10, ND-75, and NDI-100. Cells were cycles at a C/10 rate

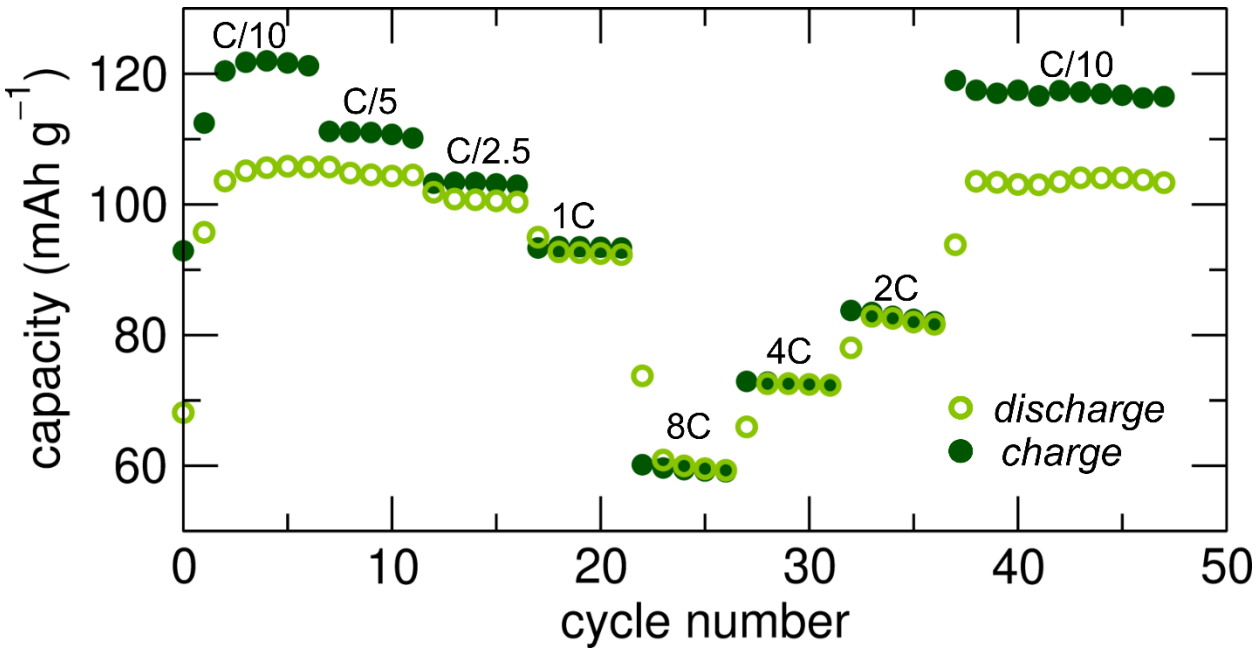

Figure S13. NDI-75 galvanostatistically cycled at variable rates from C/10 to 8C.

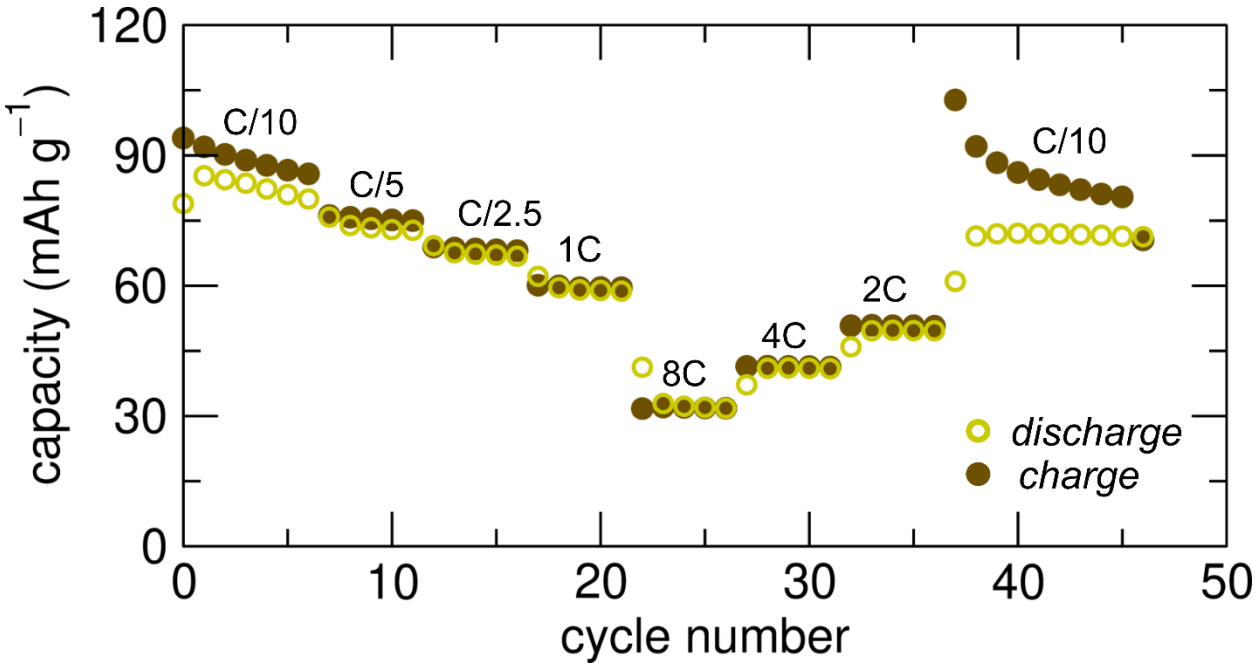

Figure S14. NDI-25 galvanostatistically cycled at variable rates from C/10 to 8C.

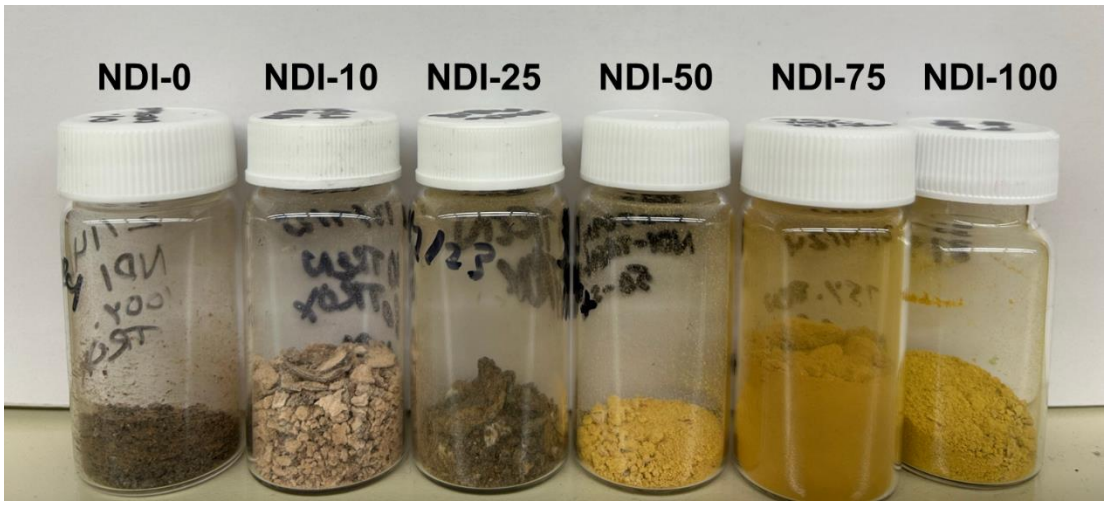

Figure S15. Photo of NDI-*X* powders.

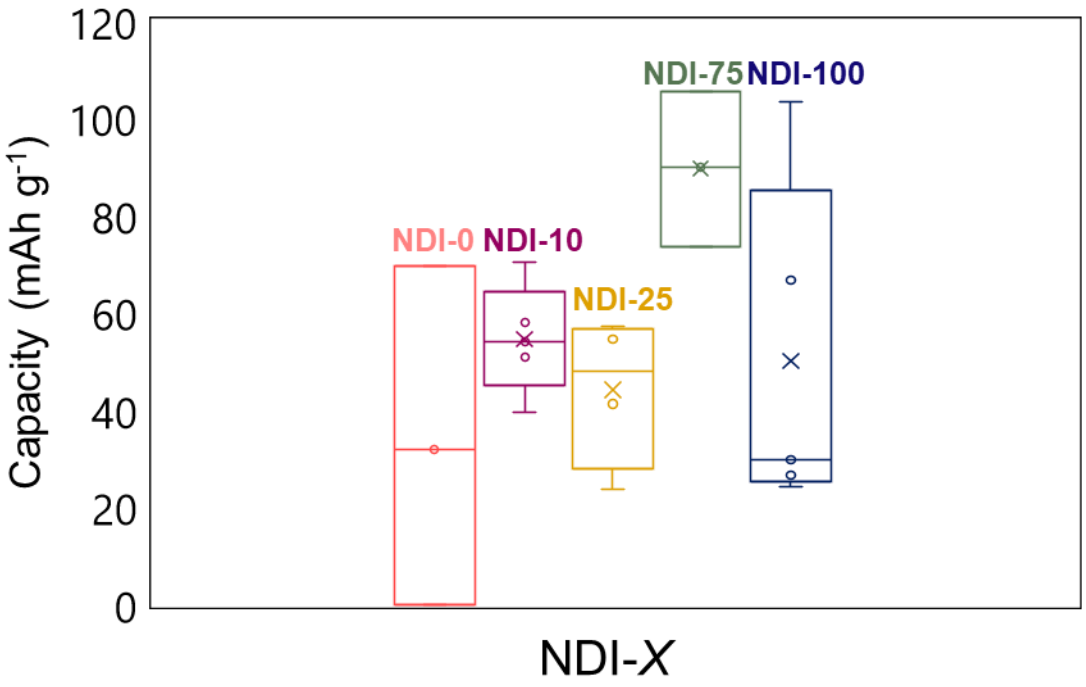

Figure S16. Box and whisker plot illustrating the variability amongst NDI-*X* coin cells

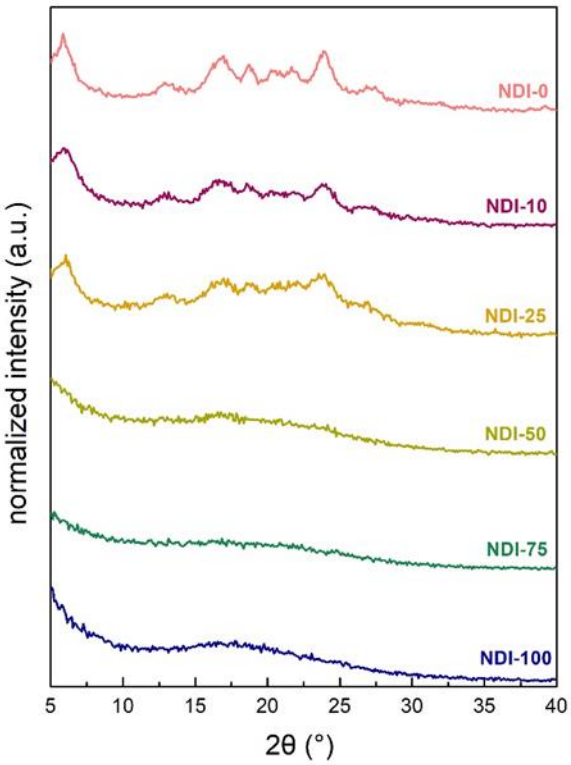

Figure S17. X-Ray Diffraction (XRD) data collected on NDI networks.

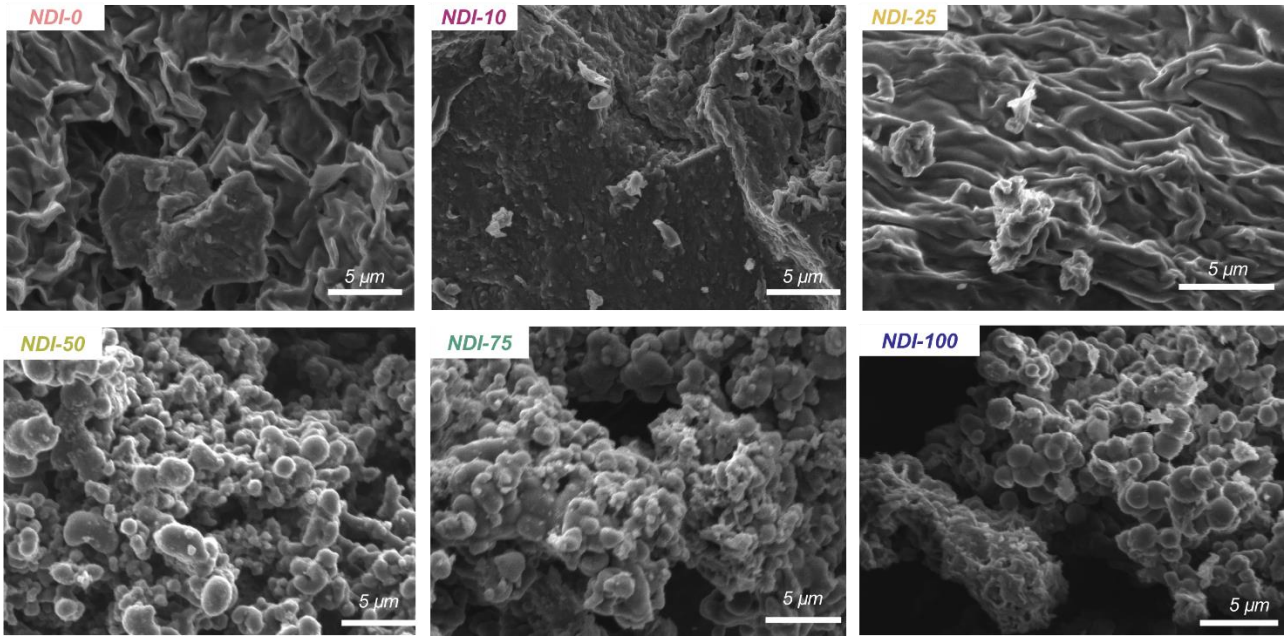

Figure S18. Scanning electron microscopy images of variably cross-linked NDI electrodes.

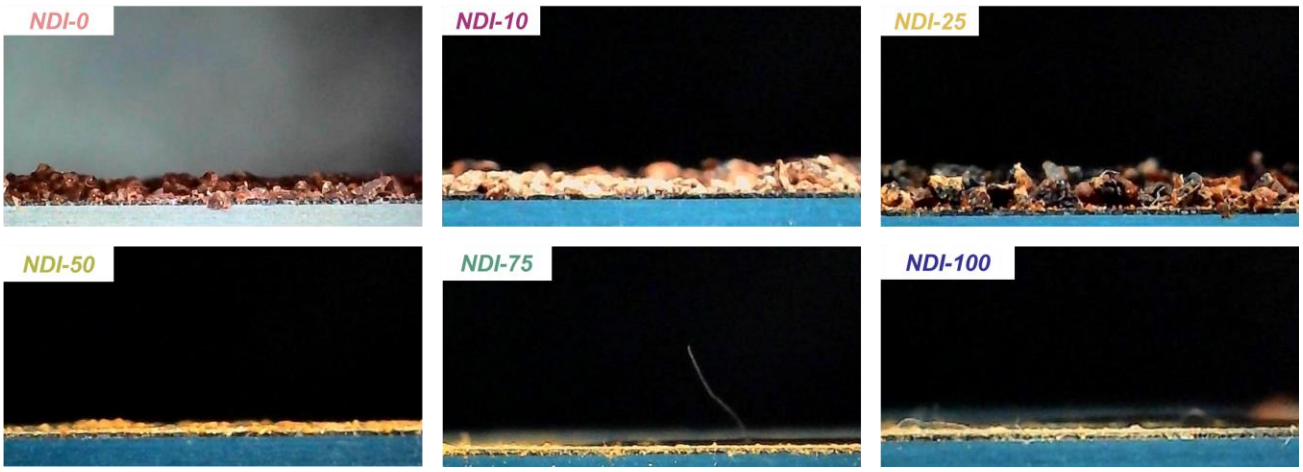

Figure S19. Contact angle experiments of NDI-X materials with 1M solution of $LiPF_6$ in ethylene carbonate: dimethyl carbonate (1:1 vol)

G. Supporting References

1. D. G. Hamilton, L. Prodi, N. Feeder and J. K. M. Sanders, *Journal of the Chemical Society, Perkin Transactions 1*, 1999, 1057-1066.
2. S. Jhulki, C. H. Feriante, R. Mysyk, A. M. Evans, A. Magasinski, A. S. Raman, K. Turcheniuk, S. Barlow, W. R. Dichtel, G. Yushin and S. R. Marder, *ACS Applied Energy Materials*, 2021, **4**, 350-356.